



The Electric Field Driven Generator

By Katsuo Sakai

Abstract- Dr. Feynman predicted it to be theoretically possible to generate electric energy from an electric field. For realizing his predict, a new electrostatic generating method was proposed by the author that uses Asymmetric electrostatic force as the driving force of a charge carrier for the generator. Therefore this generator was named the electric field driven generator.

After experimenting with many models using pendulum-type equipment, rotation-type equipment was tried.

This experimental equipment produced electricity continuously when the applied voltage to the high voltage electrode was higher than 5.8 kV. This result was estimated by a simulation, and the measured collection currents for different high voltages almost agreed with the simulated collection current. Therefore the theory of the electric field driven generator was confirmed, and Feynman's dream has become reality.

Keywords: *electrostatic generator; asymmetric electrostatic force; charge carrier; electric field driven; electric energy.*

GJCST-C Classification: J.0



Strictly as per the compliance and regulations of:



The Electric Field Driven Generator

Katsuo Sakai

Abstract- Dr. Feynman predicted it to be theoretically possible to generate electric energy from an electric field. For realizing his predict, a new electrostatic generating method was proposed by the author that uses Asymmetric electrostatic force as the driving force of a charge carrier for the generator. Therefore this generator was named the electric field driven generator.

After experimenting with many models using pendulum-type equipment, rotation-type equipment was tried.

This experimental equipment produced electricity continuously when the applied voltage to the high voltage electrode was higher than 5.8 kV. This result was estimated by a simulation, and the measured collection currents for different high voltages almost agreed with the simulated collection current. Therefore the theory of the electric field driven generator was confirmed, and Feynman's dream has become reality.

Keywords: electrostatic generator; asymmetric electrostatic force; charge carrier; electric field driven; electric energy.

I. INTRODUCTION

Today there are many kinds of electric power generators. Each has some advantages and some disadvantages. The ideal electric power generator would never produce carbon dioxide and would be safe, stable, low cost, small, and last a long time.

The well-known physicist Richard P, Feynman estimated that, in theory, getting energy from an electric field is possible; however the shape of the electric field that would make this possible has not been discovered. [1]

An electrostatic power generator that can get energy from an electric field would be the ideal electric power generator.

Nine years ago, the author discovered Asymmetric electrostatic force [2], [3], which makes generating energy from an electric field possible. This new force acts on an asymmetrically shaped conductor in a normal electric field. Retrieving energy from an electric field becomes possible when the shape of the charged conductor-not the electric field-is changed.

Several experiments were performed using pendulum-type experimental equipment [4], [5]; however, all those experiments failed.

*Author: Electrostatic Generator Laboratory Yokohama Japan.
e-mail: gy7a-ski@asahi-net.or.jp*

II. THEORY OF THE ELECTRIC FIELD DRIVEN GENERATOR

a) *Asymmetric electrostatic force*

For a long time, the main purposes of electrostatic research were electro photography and electro spray coating. Both technologies make use of charged fine powders that are moved by electrostatic force. When this electrostatic force was calculated, the charged fine powder was regarded as a point charge, and the well-known Coulomb's formula (1) was used. The magnitude of this electrostatic force doesn't change when the direction of the electric field turns over as shown in Figure 1.

$$f = qE \quad (1)$$

where f: an electrostatic force that acts on a point charge,
q: quantity of charge of a point charge;
and E: intensity of the electric field in which a point charge is placed.

The application of this formula is limited to point charges and sphere-shaped charged carriers [6].

In contrast, a new electrostatic generator that uses a non-spherical charged carrier was presented recently [7,8]. This generator uses an asymmetric shaped conductor as its charge carrier. The electrostatic force that acts on this asymmetrically shaped charged carrier was both simulated [3] and experimentally measured [2]. As a result, the magnitude of this electrostatic force was found to change when the direction of the electric field is reversed as shown in Figure 2.

This changeable electrostatic force was named as Asymmetric electrostatic force.

As shown in Figure 2, the left side of the electric field is called the forward electric field and the right side of the electric field is the backward electric field. The magnitude of the electrostatic force becomes less than half when the direction of the electric field is reversed.

b) *The basic theory of the electric field driven generator*

An electrostatic generator builds the electric charge to a high potential by mechanical force against the electric force that acts on this charge. The mechanical force cannot carry the charge directly, therefore, the charge is packed into a suitable body. We call this body the charge carrier.

Coulomb's law

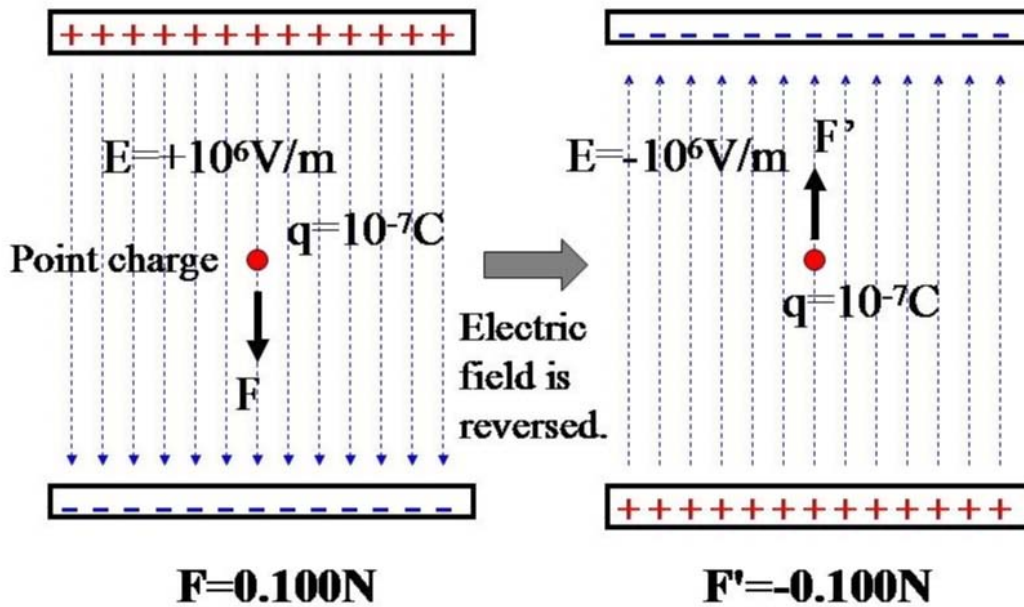


Fig. 1: Electrostatic force that acts on a point charge (Coulomb's law)

Asymmetric electrostatic force

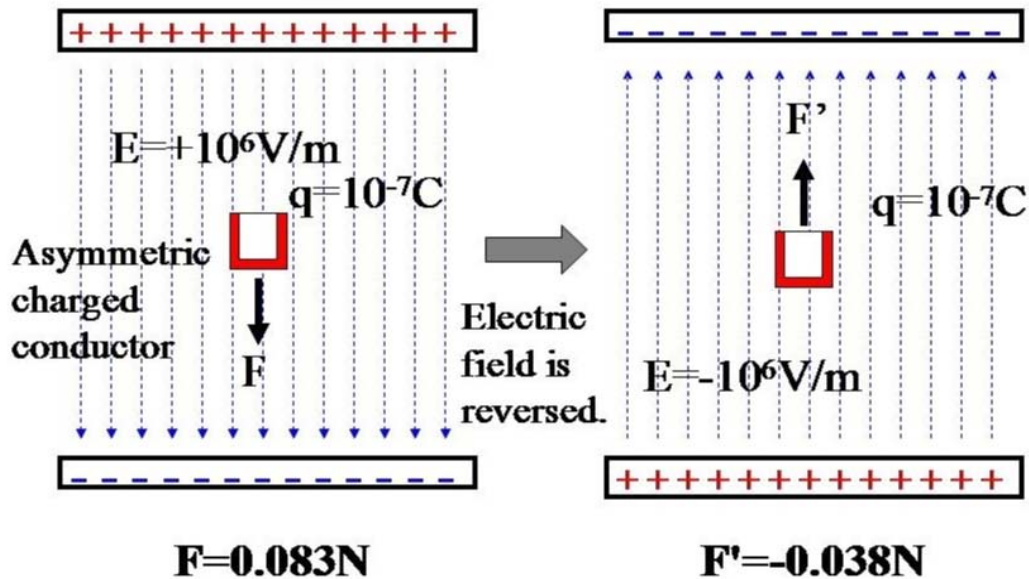


Fig. 2: Electrostatic force that acts on charged box conductor (Asymmetric electrostatic force)

The most popular electrostatic generator is the Van de Graaff electrostatic generator [9] invented by Dr. Van de Graaff in 1931. Today, it is used with a large voltage power supply and can produce ten million volts. In this machine, an insulating belt is used as a charge carrier. Figure 3 shows an example of this generator.

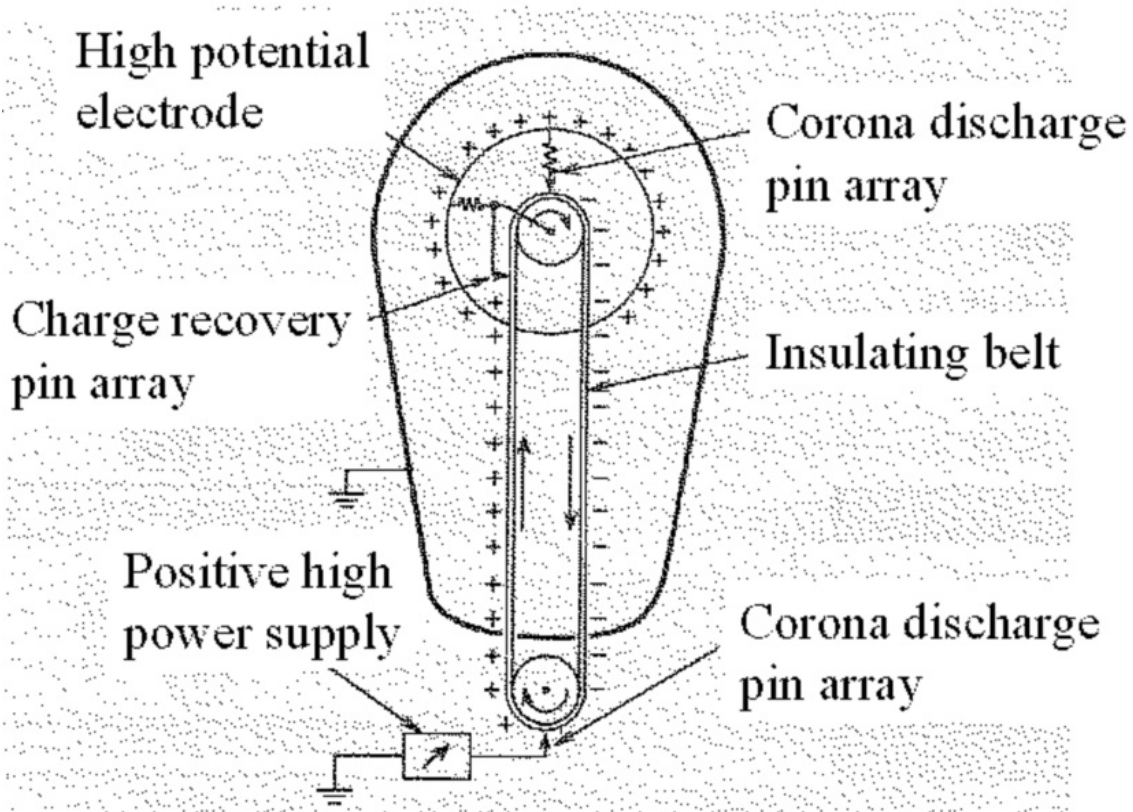


Fig. 3: Schematic layout of the Van de Graaff electrostatic generator

A motor moves the insulating belt in the direction of the arrow. The bottom corona discharge pin array places positive ions on the insulating belt. The positive ions on the insulating belt are carried to the high voltage electrode sphere by the mechanical force of a motor. Corona discharge occurs between the negative charge on the recovery pin array and the positive ions on the insulating belt. As a result, the positive ions on the insulating belt are neutralized by the negative corona ions. Then, positive charges are added to the high voltage electrode sphere.

The principle of this electrostatic generator is shown schematically in Fig. 4.

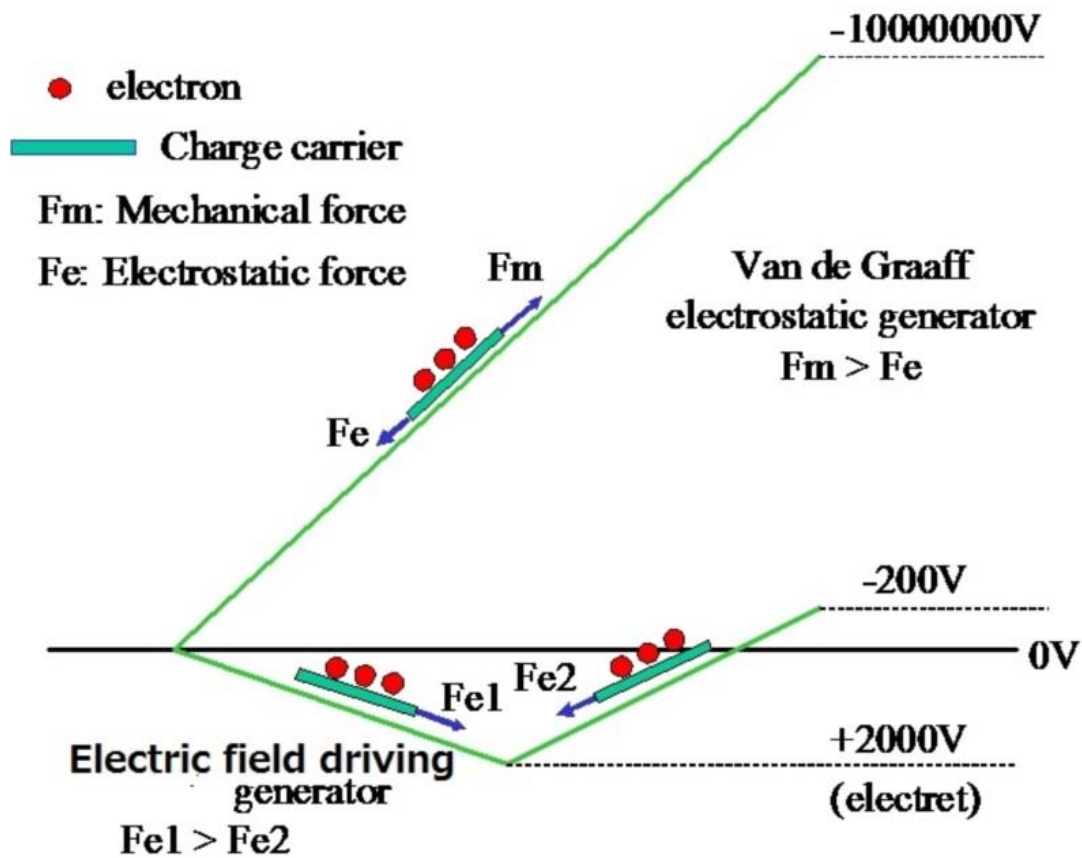


Figure 4: Schematic explanation of the principles behind the two electrostatic generators theory.

In Figure 4, the bold green line represents the potential, and the blue arrows represent the forces. The small red circles represent electrons, and the sky blue plates represent the charge carriers. In the Van de Graaff electrostatic generator, the charge carriers are directly transported by a strong mechanical force, F_m , against the electrostatic force, F_e .

In contrast, in the electric field driven generator, the charge carrier is first moved to the forward electric field caused by the high voltage source (electret) according to the electrostatic force F_{e1} . In this process, the charge carrier gains kinetic energy from the electric field. Then, the charge carrier is moved into the backward electric field, expending the given energy against electrostatic force F_{e2} .

The shape of this charge carrier is asymmetric. Therefore, asymmetric electrostatic force acts on this charge carrier. Thus, the absolute value of F_{e1} is larger than that of F_{e2} . As a result, the charge carrier can arrive at a potential (-200V) that is higher than the initial potential (0V).

The basic unit of the electric field driven generator that is driven by asymmetric electrostatic force is concretely shown in Figure 5.

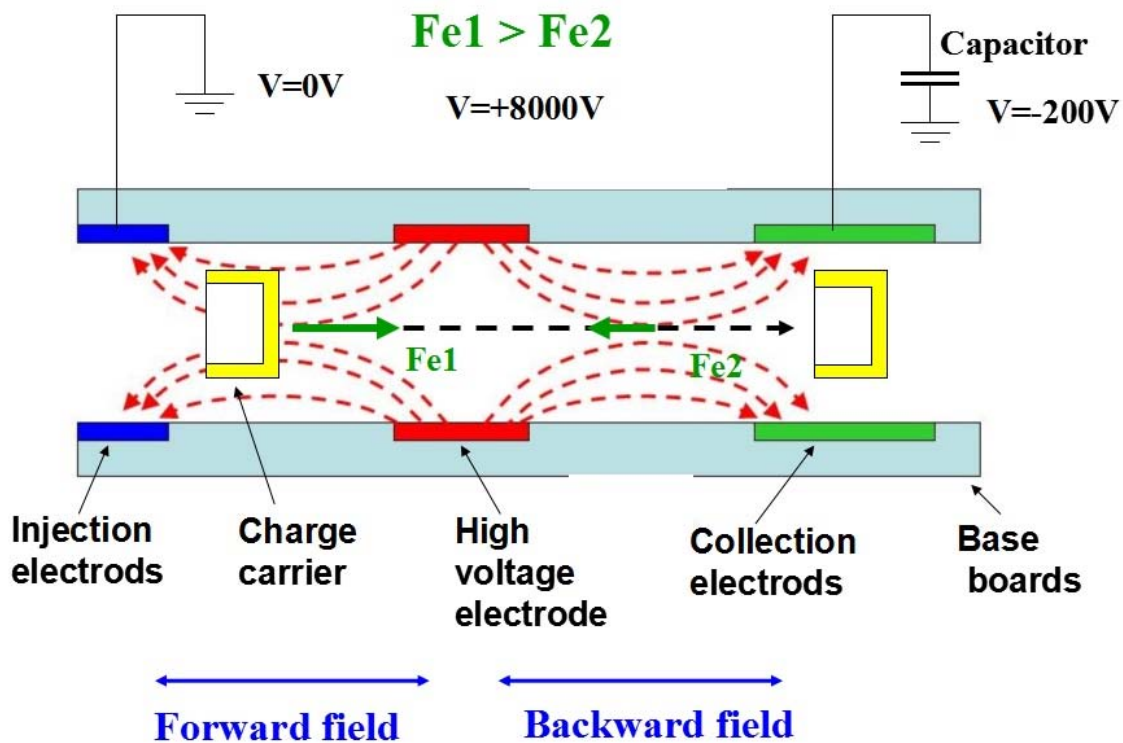


Figure 5: Schematic layout of a basic unit of the electric field driven generator

The generator in Figure 5 mainly consists of charge injection electrodes, high voltage sources, charge collection electrodes, and charge carriers. The electrodes and the high voltage source are positioned on an insulating base board.

The high voltage source gives a positive high voltage. The injection electrodes are grounded. The collection electrodes are kept at a negative low voltage. As a result, the high voltage source and the injection electrodes produce a forward electric field for a negative charge between them. The high voltage source and the collection electrodes produce a backward electric field for a negative charge between them. The line of electric force is depicted as red arrow dotted lines in Figure 5.

A gutter shape conductor is used as a charge carrier that carries negative charge (electron) from the injection electrodes to the collection electrodes through the high voltage sources.

Asymmetric electrostatic phenomenon produces a large electrostatic force in the forward electric field and it produces a weak electrostatic force in the backward electric field. Therefore, the charge carrier gains a large amount of kinetic energy in the forward electric field. Then, it loses some of its kinetic energy in the backward electric field. As a result, the charge carrier maintains extra kinetic energy when it arrives at the collection electrodes. The carried charge can be built to a higher potential by this extra energy. This result means that the equipment described by fig.5 can produce an electric energy. Namely this equipment is the new electrostatic generator.

The just above mentioned explanation is the principle of the electric field driven generator. This principle is different from that of the Van de Graaff electrostatic generator.

III. EXPERIMENT INSTRUMENT

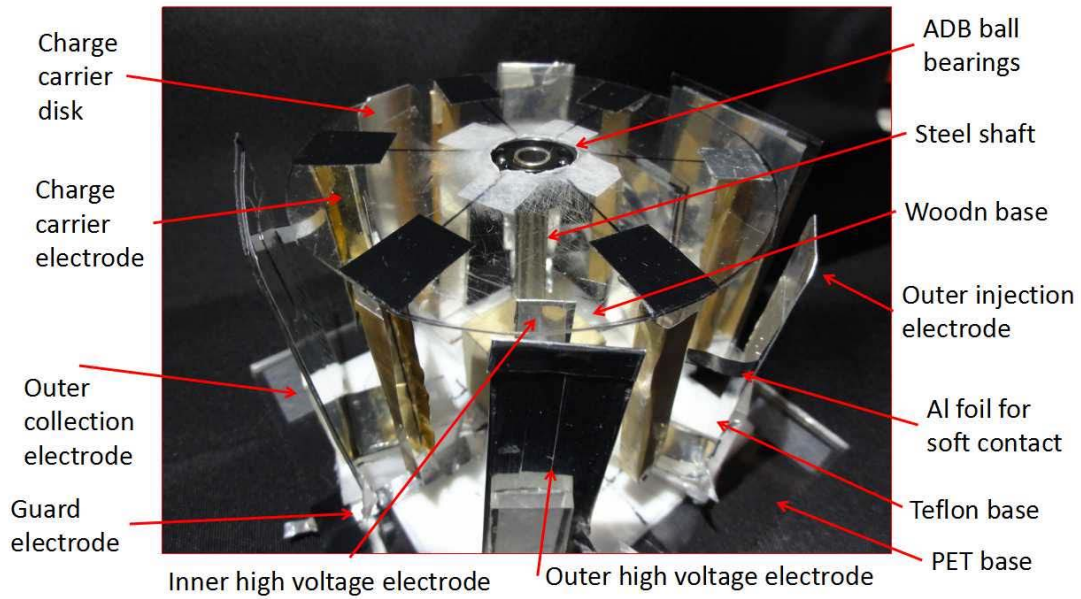


Figure 6: A photograph of the main part of the experiment equipment of the electric field driven generator

Figure 6 shows a photograph of the main part of the experimental equipment. Figure 7 shows the front view on the dotted line of Figure 8, and Figure 8 shows an aerial view of the experiment equipment.

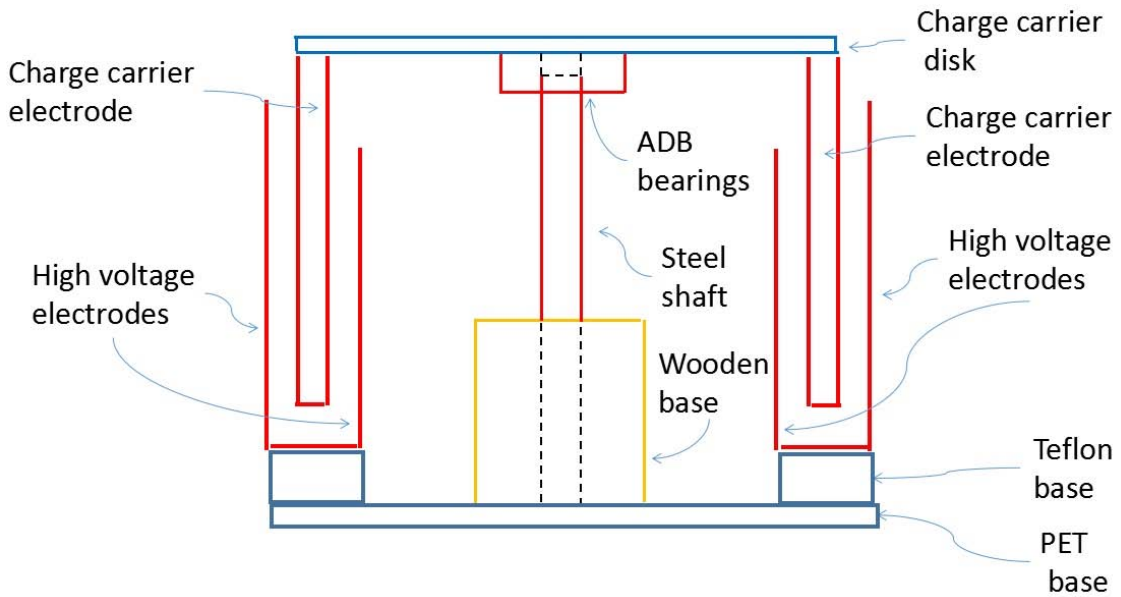


Figure 7: Front view of the experiment equipment of the electric field driven generator



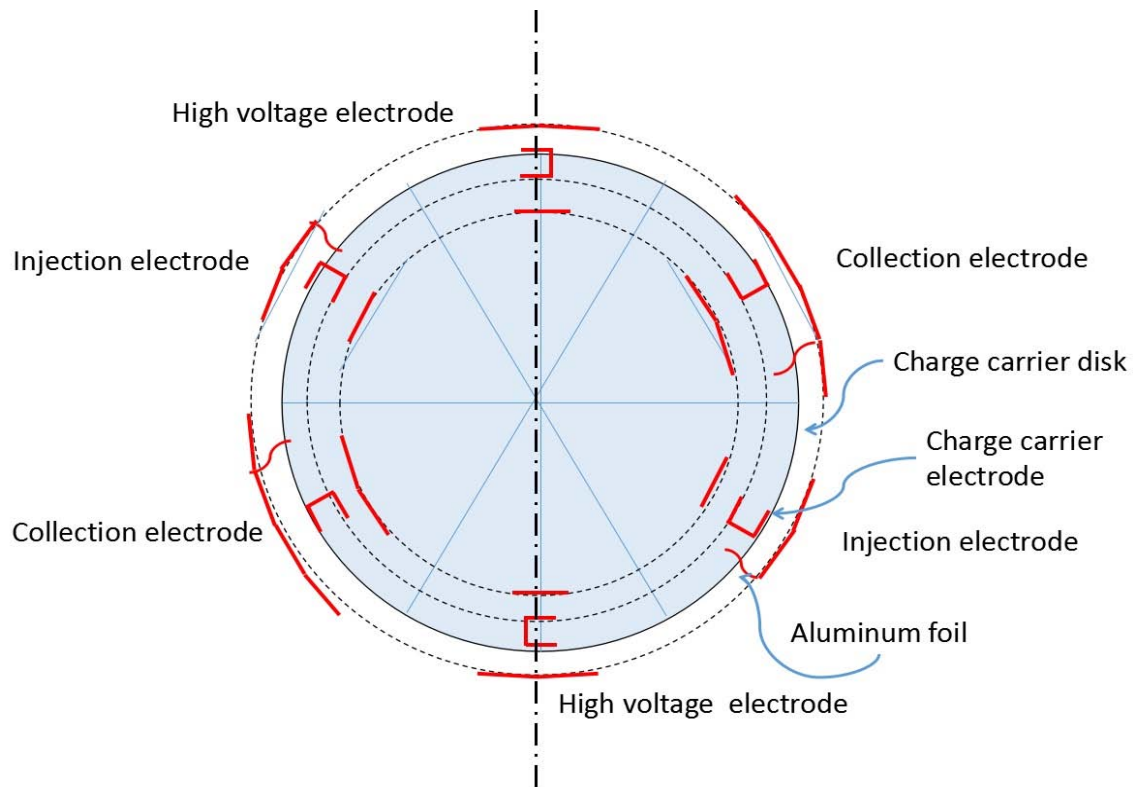


Figure 8: Aerial view of the experiment equipment of the electric field driven generator

This equipment mainly consists of two charge injection electrodes, two high voltage electrodes, two charge collection electrodes, a charge carrier that has a disk and six charge carrier electrodes, and four electric terminals.

The charge carrier disk is a 0.5 mm thickness PET plate with a diameter of 100 mm. ADB (Autonomous Decentralized Bearing) bearings were fixed on the center of the disk. The ADB bearing can rotate easily around the steel shaft because the kinetic friction coefficient is only 0.0015.

The six charge carrier electrodes were placed at 60-degree intervals as shown Figure 8. The charge carrier electrodes were made from double-sided gold-plated aluminum plates with 0.1 mm thicknesses. The electrostatic force always acts on the gold surfaces perpendicularly. The charge carrier electrode was created in a gutter shape with a height of 60 mm and width and breadth of 5 mm each. The total weight was only 1.4 g.

The two charge injection electrodes, two high voltage electrodes, and two charge collection electrodes were placed on the main PET base plate at 60-degree intervals as shown in Figure 8. Each electrode was placed on a Teflon base to reducing the leak current as shown in Figure 7.

Those six electrodes had an outer electrode and inner electrode, and the distance between them was 20 mm. The injection electrodes and the high voltage electrodes were made from aluminum plates with 0.1 mm thicknesses. The collection electrodes were

made from aluminum plating with 0.1 mm thickness and PET film with 0.5 mm thickness. The electrodes consisted of three layers: aluminum plate, PET film, and aluminum plate. As a result, it became a capacitor. This small capacitor was connected to the big outer capacitor (not shown in Figure 8). The size of this capacitor was 20cm by 20cm as was required by the surface potential meter. The capacitance of the small capacitor became 330 pF, and the capacitance of the big capacitor became 1100pF because the relative permittivity of PET is 3.2. The total capacitance of the two capacitors was 1430pf. Hereafter those two capacitors are together called the collection capacitor or, simply, the capacitor.

The height of the outer electrodes was 60 mm, and the height of the inner electrodes was 50 mm. The width of the outer injection electrode, the outer high voltage electrode, and the outer collection electrode were 22 mm, 22 mm, and 44 mm, respectively. The width of the inner injection electrode, the inner high voltage electrode, and the inner collection electrode were 10 mm, 10 mm, and 20 mm, respectively. The distance between the outer injection electrode and the outer high voltage electrode and the distance between the outer high voltage electrode and the outer collection electrode were 30 mm each. The distance between the inner injection electrode and the inner high voltage electrode and the distance between the inner high voltage electrode and the inner collection electrode were 25 mm each.

The injection electrodes were always grounded, the high voltage electrodes were connected to a high voltage power supply, and the surface potential of the collection capacitor was measured by a surface potential meter.

The injection electrodes and the collection electrode had aluminum foil on the inner surface as an electric connector as shown in Figure 8. The width was 5mm, and the length was 10mm. The foils softly connected the charge carrier electrode to the injection and collection electrode electrically.

The collection electrodes were wide. As a result, the collection electrodes could perform semi-Faraday gauge. When the charge carrier electrode was connected to the collection electrode by the aluminum foil, more than 90% charge on the charge carrier electrode was transferred to the collection electrode (simulation result).

Grounded aluminum slices (10mm x 100mm) were located just before the collection electrode. The

leak current from the high voltage electrode to the collection electrode was captured here.

The surface potential meter (SHISHIDO ELECTROSTATIC: STATIRON-DZ 3) was used to measure the surface potential of the collection capacitor.

IV. SIMULATION RESULT

Four kinds of forces act on the moving charge carrier that consisted of a disk and six electrodes as shown in Figure 9. The forces are the electrostatic force, the kinetic friction force, the mechanical resistance force of the aluminum foil, and the air resistance force. The electrostatic force, the mechanical resistance force, and the air resistance force act on the charge carrier electrodes and the kinetic friction force acts on the rotating charge carrier disk and the ADB bearings.

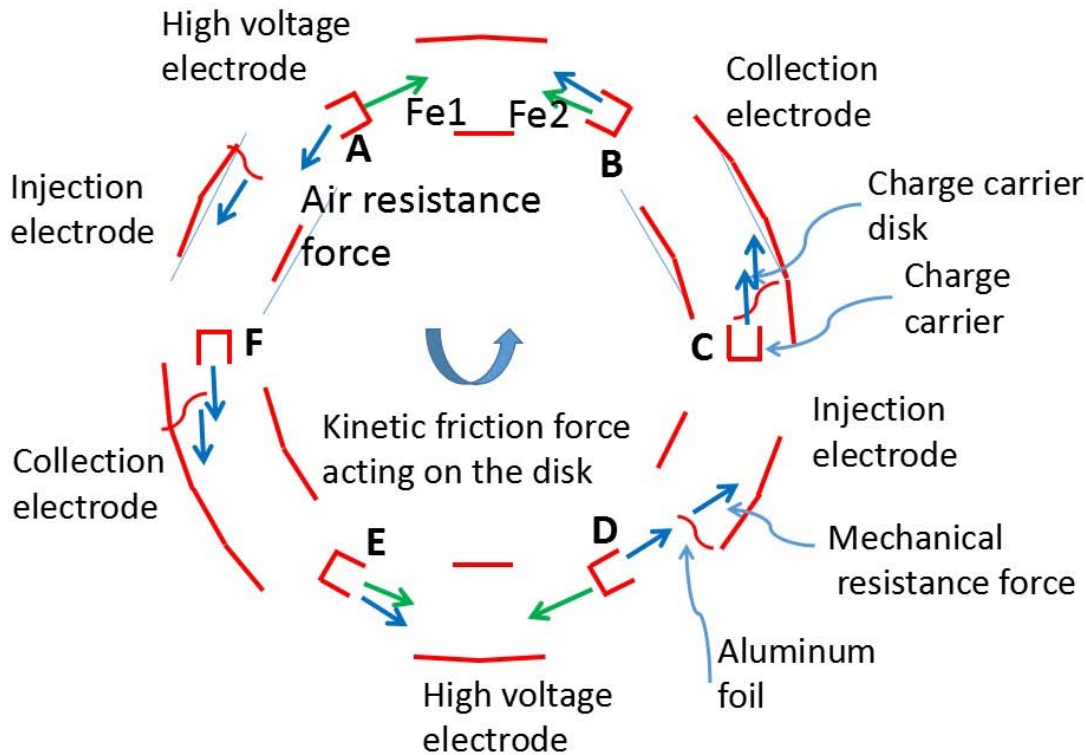


Figure 9: Four kinds of force that act on the moving charge carrier

At first, the electrostatic force is simulated. In Figure 9, the charge carrier electrodes A and D are accelerated by a forward electrostatic force Fe_1 in the forward electrostatic field between the injection electrode and the high voltage electrode. At the same time, charge carrier electrodes B and E are decelerated by a backward electrostatic force Fe_2 in the backward electrostatic field between the high voltage electrode and the collection electrode. On the contrary side, the charge carrier electrodes C and F do not suffer any electrostatic force because there is no electric field in

the area from the collection electrode to the injection electrode.

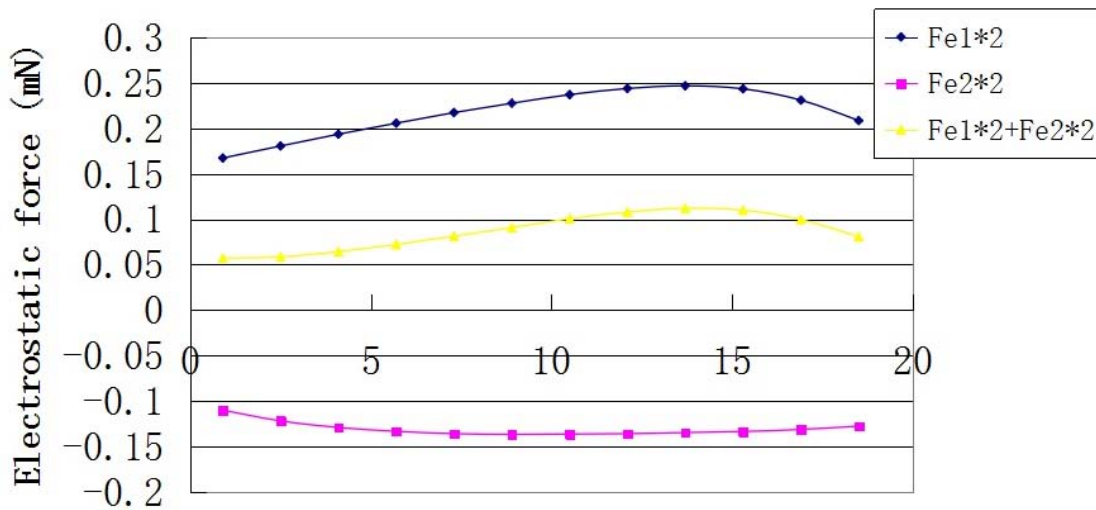
As a result, the total electrostatic force that acts on those six charge carrier electrodes is calculated by the following equation (2).

$$F_{et} = Fe_1 \times 2 + Fe_2 \times 2 \quad (2)$$

where F_{et} : total electrostatic force,
 Fe_1 : accelerating electrostatic force,
 and Fe_2 : decelerating electrostatic force.

Fe1 and Fe2 were simulated by the two-dimensional finite difference method. Figure 10 shows

the simulation result of Fe1 and Fe2 when the high voltage was 6.0kV.



Distance from injection and high voltage electrode (mm)

Figure 10: Simulation results of Fe1 and Fe2

According to Figure 10, the average of the total electrostatic force Fe1*2+Fe2*2 is about 0.086 mN. Therefore the total of the air resistance force, the mechanical resistance force, and the kinetic friction force must be lower than 0.086 mN.

Next, the air resistance force: Fa is calculated by the following equation (3).

$$Fa = (Cd \times \rho \times S \times v^2) / 2 \quad (3)$$

where Cd: air resistance coefficient,
 P : air density,
 S: front surface area of the charge carrier electrodes,
 and v: velocity of the charge carrier electrode.

The air resistance coefficient varies with the shape of the moving body. The value for the gutter-shaped charge carrier electrode was decided as 1.5 because the shape looks like a square pillar that has a round edge. Air density is 1.3 kg/m³. The front surface area of the charge carrier electrode is 0.0018 m² because the breadth is 5.0 mm and the height is 60.0 mm. The velocity of the charge carrier electrode is 0.157 m/s, because the RPM (rotation per minute) is 30 for minimum stable rotation of the charge carrier, and the radius of the charge carrier disk is 0.05 m.

As a result, the air resistance force becomes 0.043 mN. This value is half of the electrostatic force. Therefore if the total force of the remaining two forces is about 0.043mN, the charge carrier disk will rotate

continuously when the high voltage electrode was applied +6.0kV.

Third, the mechanical resistance force of the aluminum foils is roughly estimated, because the exact simulation of this force is very difficult.

The mechanical force that accelerates a piece of aluminum foil from 0 m/s to 0.157 m/s in the distance 5.0 mm was calculated with the kinetic equations. The width of the piece is 5.0 mm, the length of the piece is 5.0 mm, and the weight of the piece is 0.0008125 g. As a result, the force becomes 2.0μN. There are four pieces in one round; therefore each charge carrier electrode accepts 8.0μN. There are six charge carrier electrodes on a charge carrier; therefore the total force that acts on the charge carrier electrodes is 0.048 mN.

Finally, the kinetic friction force was estimated. The kinetic friction coefficient of the ADB bearings is only 0.0015, and the weight of the charge carrier was only 7.7g.; therefore the kinetic friction force will be almost zero.

As a result, the total force of the air resistance force, the mechanical resistance force, and the kinetic friction force is roughly estimated as 0.091mN. This total force is about the same as with the electrostatic force: 0.086mN.

Therefore, the charge carrier can be expected to rotate continuously and generate electricity when the high voltage electrode is applied +6.0kV or a little higher.

V. RESULTS

The high voltage electrode was applied from +5.6kV to +9.4kV by the interval 0.2kV, and the movement of the charge carrier rotation and the surface potential meter display was taken by the digital camera (Sony Cyber-shot DSC-HV5V).

When the applied voltage was +5.6kV, the charge carrier could not rotate continuously, and when the applied voltage was +9.4kV, a corona discharge occurred. When the applied voltage was +5.8kV to +9.2kV, the charge carrier could rotate continuously and the surface potential changed from 0.00kV to -0.3 ~ -0.6kV.

One example of those measurements are shown in Figure 11. The applied voltage was +8.0kV.

At first, the surface potential quickly increases in a negative direction. However, the increase rate gradually slows. After 600 seconds, the increase rate becomes almost zero. This increased rate of the surface potential is proportional to the collection (generating) current; it is the electric power generating rate. However, these results do not mean that the electric power generation became zero after 600 seconds rotation because after 1200 seconds of rotation, the surface potential increased again rapidly to a negative direction when the upper aluminum plate of the collection capacitor was instantaneously grounded. This result means that the electric power generates anytime after the capacitor is emptied.

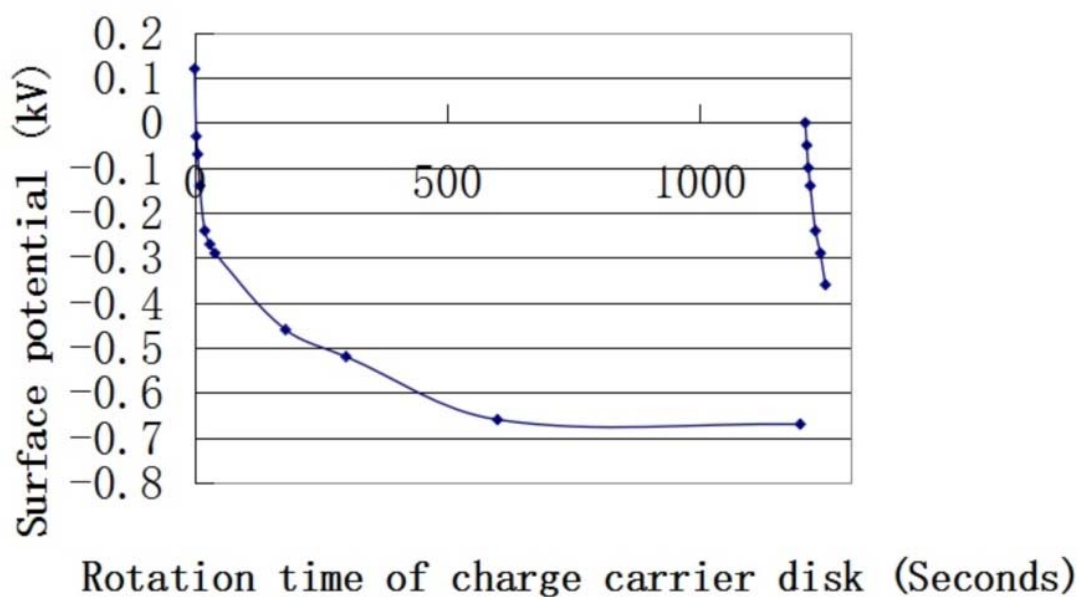


Figure 11: The surface potential change of the collection capacitor for the rotation time of the charge carrier disk

The increasing rate of the surface potential when 8.0 kV was applied at 0 second, and the increasing rate when the capacitor was grounded at 1200 second, were almost the same, as shown in Figure 11.

The collection current can be calculated with this surface potential change and the capacity of the collection capacitor (1430pF).

Therefore, the collection currents for different high voltages were calculated by measuring the surface potential change when the capacitor was grounded. The measurements were taken three times for each high voltage, and an average collection current was calculated.

When 7.0kV was applied to the high voltage electrode, the charge carrier started to rotate automatically and the surface potential changed as shown in Figure 12.

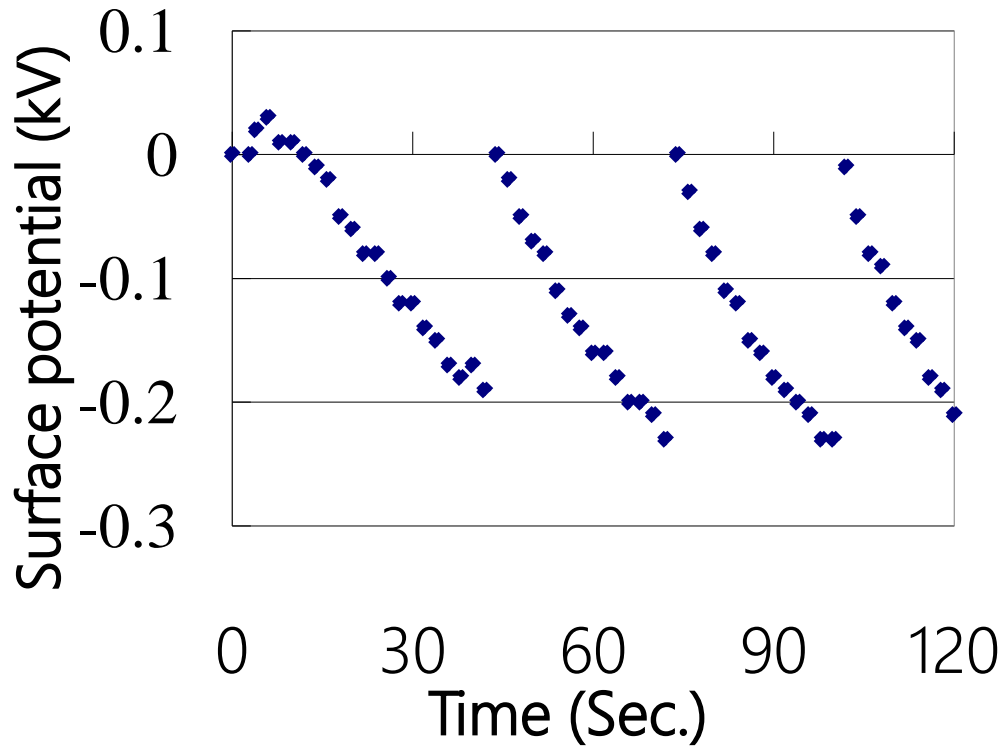


Figure 12: The surface potential change of the collection capacitor when the capacitor was grounded

When 7.0kV was applied at 0 second, the surface potential shows +0.04kV as shown in Figure 12. This +0.04kV is an induced surface potential because the upper electrode of the capacitor is electrically floating between the high voltage electrode and the grounded lower electrode of the capacitor.

However, when the upper electrode of the capacitor was grounded at 45 second, this induced surface potential was not recognized. This result is because the charge carrier disk was rotating rapid at this time therefore the negative collection current canceled the positive induced potential quickly.

The increase rate of the collection currents after grounding was fast. On the other hand, the increased rate of the collection current when 7.0kV was applied at 0 second was slow. This result is because the rotation speed of the charge carrier disk increases gradually from 0 second, and the rotation speed became constant when the upper electrode of the capacitor was grounded at after 40 second.

Figure 13 shows the measured average collection current for different high voltages.

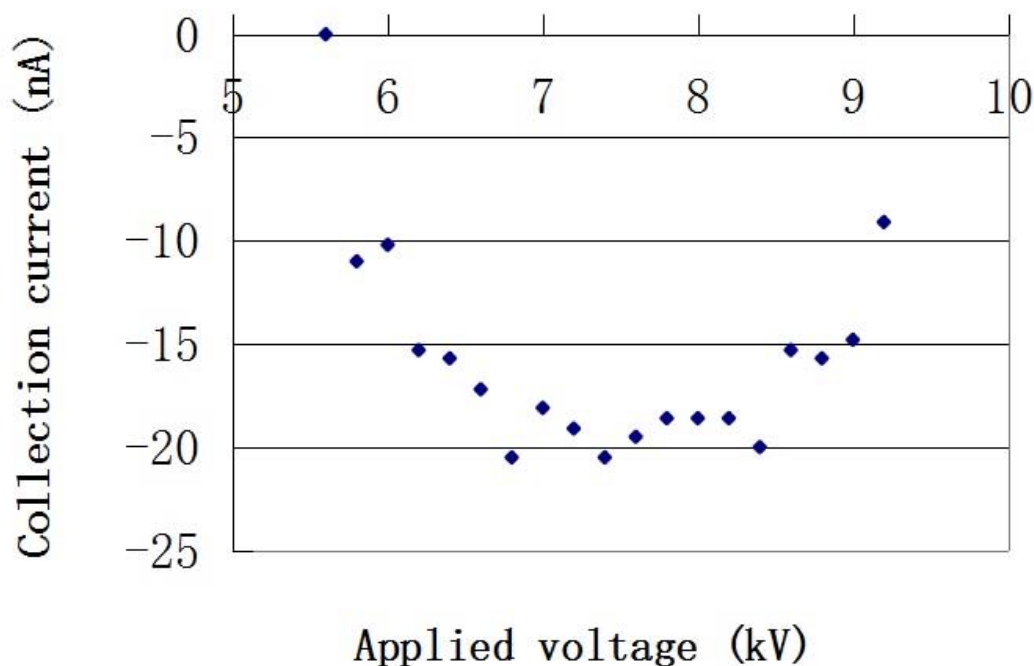


Figure 13: The measured collection current for different high voltages

Figure 13 demonstrates that the collection current almost increases in proportion with an applied high voltage, that is, generated electricity is in proportion to an applied high voltage. However, when the high voltage is higher than 8.0kV, the collection current becomes saturated and reduced. This cause will be considered in the next section.

Incidentally, when the applied high voltage was lower than 6.8kV, the charge carrier disk could not start to rotate automatically because the electrostatic force is lower than Static frictional force, so an air flow assisted the disk in starting rotation at first. After starting to rotate it can rotate continuously because the electrostatic force is higher than the Kinetic friction force.

VI. DISCUSSION

In theory the collection current increases with the applied voltages. However, the measured collection current decreased when the applied voltage was higher than 8.0kV as shown in Figure 13. This unexpected result is because of the leak current that flows from the high voltage electrodes to the collection electrodes.

The polarity of the leak current is positive, but the collected charge in the capacitor is negative. Therefore, the collected charge was partly canceled. The grounded guard electrodes just before the collection electrodes can cut the surface leak current. However, they cannot cut the volume leak current.

Figure 14 shows the measured leak current.

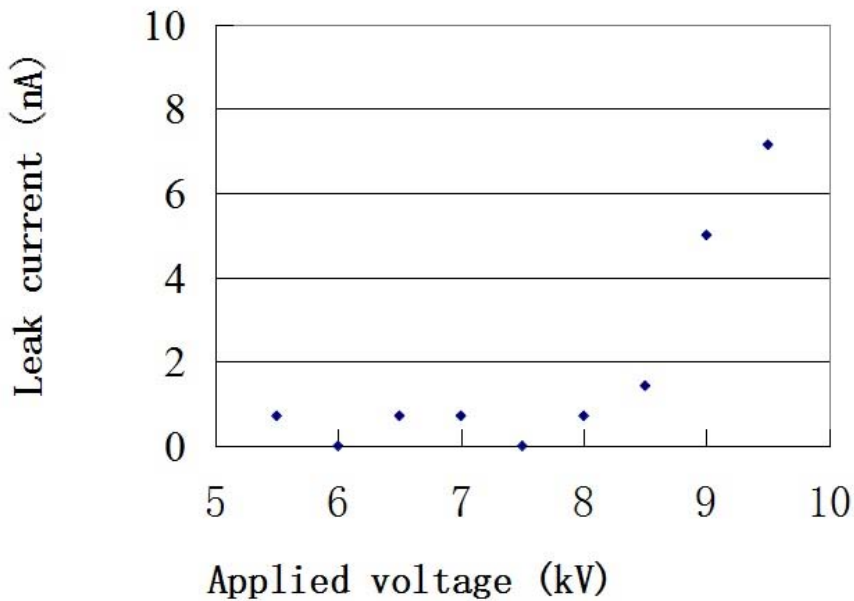


Figure 14: The leak current that flows into the collection electrode for different applied voltages

The leak currents were calculated from the surface potential increase 10 seconds after the capacitor was grounded.

When the applied voltage is lower than 8.0kV, the leak current is almost zero. However, it rapidly increases from 8.0kV as shown in Figure 14.

Figure 15 shows the measured collection current and the measured leak current simultaneously.

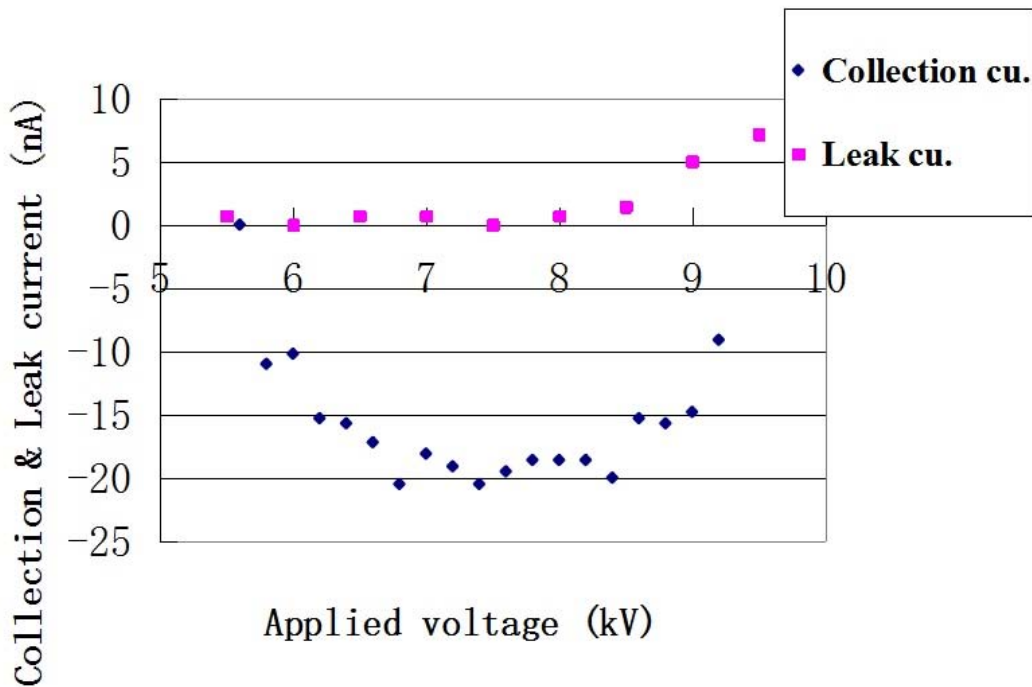


Figure 15: The measured collection current and the measured leak current for different high voltages

Figure 15 demonstrates a decrease of the collection current over 8.0kV because of the leak current increases over 8.0kV.

The collection current can be calculated by the following equation.

$$A = q \times r \times R \times n \times m \quad (4)$$

where q: injected charge quantity from the injection electrode to the charge carrier electrode,

r: charge collection rate from the charge carrier electrode to the collection electrode,

n: number of the collection electrode,

m: number of the charge carrier electrode, and

R: rotation number of the charge carrier disk per minute.

The injected charge quantity q from the injection electrode to the charge carrier electrode was decided by

a simulation. For example, it became 1.2 nano-Coulombs when the applied voltage was +6.0 kV.

The simulation result of the charge collection rate "r" from the charge carrier electrode to the collection electrode was more than 0.9. However, 0.9 was used because the actual equipment was a little different from the simulated equipment.

The number n of the collection electrode was two, and the number m of the charge carrier electrode was six.

The rotation number R of the charge carrier disk per minute (RPM) was counted from the experiment movie. Figure 16 shows the counted RPM.

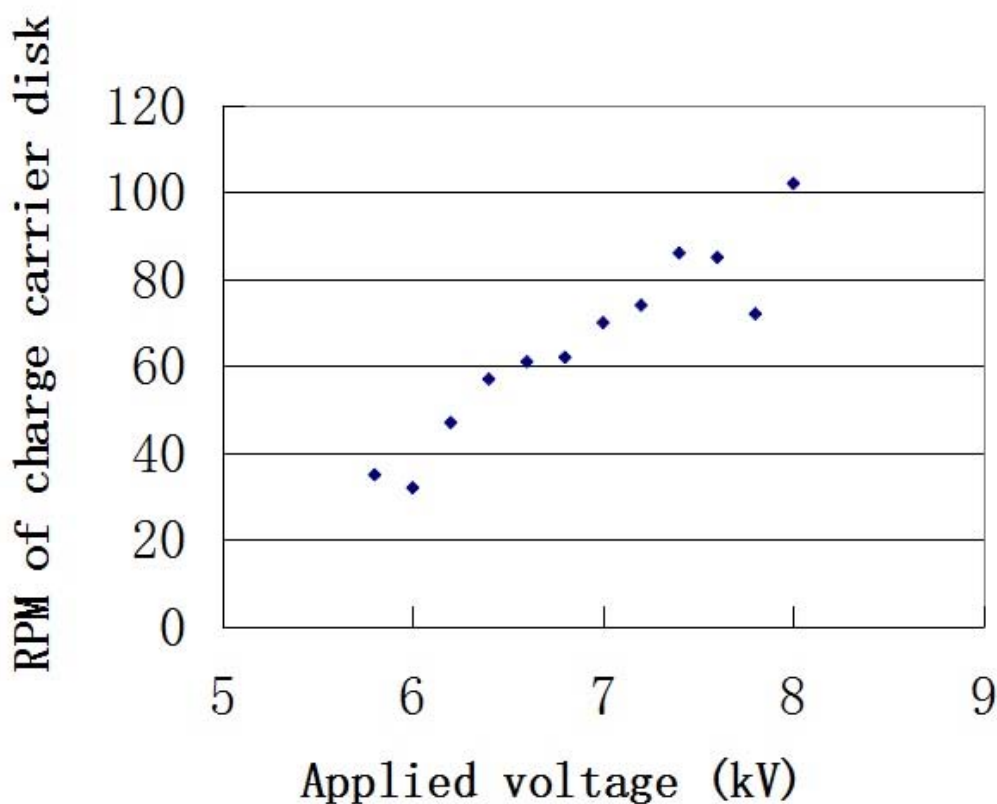


Figure 16: The RPM of the charge carrier disk for different high voltages

The calculated collection current when the applied voltage was lower than 8.0kV is shown in Figure 17 with the measured collection current.

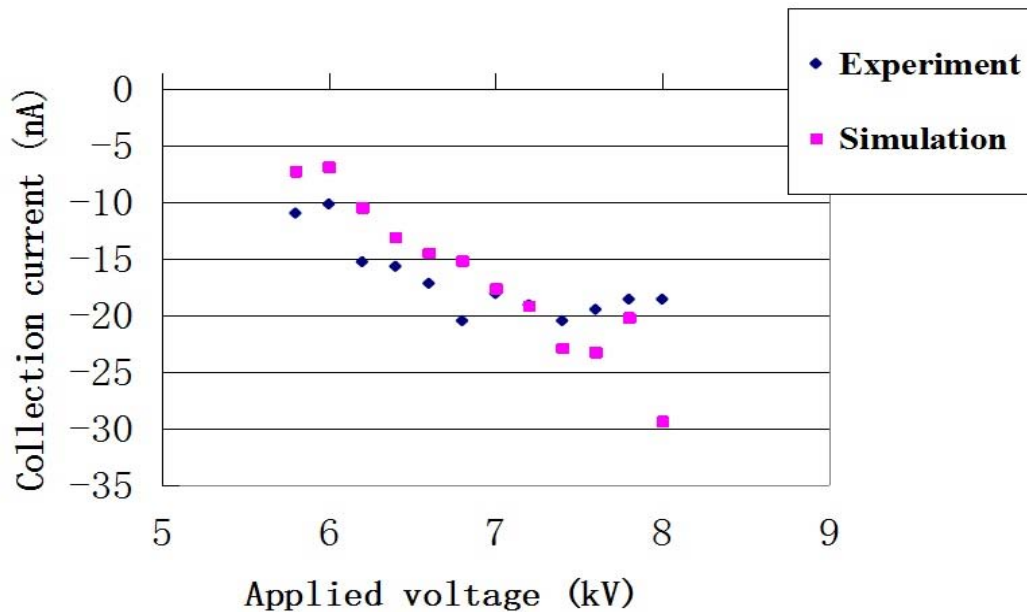


Figure 17: The simulated collection current and the measured collection current for different high voltages

Figure 17 shows that when the applied voltage is lower than 8kV, the calculated collection current almost agrees with the measured collection current. The small difference between the experiment and the simulation may be because of a small difference between the real value and the estimated value of the injection charge quantity and the collection rate.

The lowest high voltage that can rotate the charge carrier continuously was estimated by the simulation as about +6.0kV. The actual lowest high voltage was +5.8kV, and the measured collection current agreed with the calculated collection current. Those results mean that the theory of the electric field driven generator is correct and this experimental equipment produced electricity: Electric energy could be produced from an electric field.

VII. CONCLUSION

This experiment confirmed that the experimental equipment of the field driven electrostatic generator that uses Asymmetric electrostatic force as a driving force of the charge carrier can generate electricity continuously. Namely Electric energy was gained from an electric field. This experimental result may be the first successful attempt at this in the world.

The experimental equipment produced the electric field with a high voltage electrode and an electric power supply. This system was used to confirm the new theory of the electrostatic generating method.

However, this system cannot be used as a commercial machine because the electric field must be produced by an electret in place of an electrode and a power supply. As a result, the electret power generator not only does not produce CO₂ but also is safe, low cost, small, lightweight, and has a long life span.

REFERENCES RÉFÉRENCES REFERENCIAS

1. Richard P. Feynman, Robert B. Leighton, Matthew L. Sands, The Feynman LECTURES ON PHYSICS Japanese version chapter 4 Electrostatics, p.44 IWANAMI publishing company.
2. K. Sakai, "Asymmetric electrostatic force", Journal of Electromagnetic Analysis and Applications 2014 on the Special Issue on Electromagnetic Field Theory, p.253-p.268
3. K. Sakai, "Theory of Asymmetric electrostatic force", Journal of Electromagnetic Analysis and Applications 2017.
4. K. Sakai, "A first trial for the new electrostatic generator that will solve the CO₂ problem", Proceedings of 2014 ESA annual Conference (2014) B3
5. K. Sakai, "A second trial for the new electrostatic generator that is driven by Asymmetric electrostatic force ", Proceedings of 2016 Electrostatics Joint Conference (2016) P4
6. David Halliday, Robert Resnick, Jearl Walker, Fundamentals of Physics. 6th edition Japanese version Chapter "Electric Charge" question 1, Wiley & sons. Inc.
7. K. Sakai, et al., Electrostatics: Theory and Applications, first ed. Nova Science Publish, New York, 2010 (Chapter 1)
8. K. Sakai, Asymmetric Electrostatic Forces and a New Electrostatic Generator, first ed. Nova Science Publish, New York, 2010.
9. Handbook of electrostatic, Japan, (1998) p.962.